ACS APPLIED BIO MATERIALS

www.acsabm.org Article

Hyaluronic Acid Oligomer Immobilization as an Angiogenic Trigger for the Neovascularization of TE Constructs

Ana L. Silva, Pedro S. Babo,* Márcia T. Rodrigues, Ana I. Gonçalves, Ramon Novoa-Carballal, Ricardo A. Pires, Jeroen Rouwkema, Rui L. Reis, and Manuela E. Gomes*

Cite This: *ACS Appl. Bio Mater.* 2021, 4, 6023−6035 Read Online

ACCESS | Metrics & More | Article Recommendations | Supporting Information

ABSTRACT: Tissue engineered (TE) substitutes of clinically relevant sizes need an adequate vascular system to ensure function and proper tissue integration after implantation. However, the predictable vascularization of TE substitutes is yet to be achieved. Molecular weight variations in hyaluronic acid (HA) have been pointed to trigger angiogenesis. Thus, this study investigates HA oligomer immobilization as a promoter for TE construct vascularization. As a proof-of-concept, the surface of methacrylated gelatin (GelMA) hydrogels were functionalized with high molecular weight (HMW; 1.5 to 1.8 MDa) and low molecular weight (LMW; < 10 kDa) HA, previously modified with aldehyde groups to enable the immobilization through Schiff's base formation. The ability of A-HA to bind amine-presenting surfaces was confirmed by Surface Plasmon Resonance (SPR). Human Umbilical Vein Endothelial Cells (HUVECs) seeded over hydrogels functionalized with LMW HA showed higher proliferation and expression of angiogenic markers (KDR and CD31), than those grown in HMW HA conjugated- or plain surfaces, in line with the activation of HA ERK1/2 mediated downstream signaling. Moreover, when cocultured with human dental pulp cells (hDPCs) encapsulated into the GelMA, an increase in endothelial cell migration was observed for the LMW HA functionalized formulations. Overall LMW HA functionalization enhanced endothelial cell response showing potential as an angiogenesis inducer for TE applications.

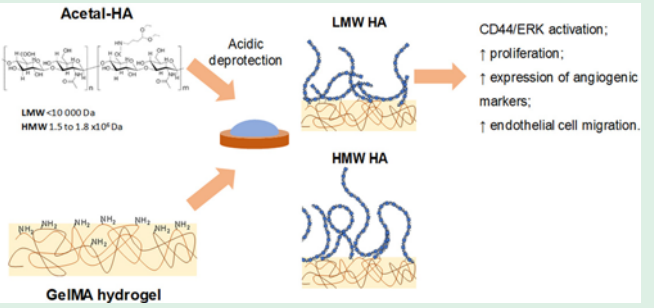

KEYWORDS: *tissue engineering, hyaluronic acid oligomers, vascularization, angiogenesis, dental pulp regeneration*

1. INTRODUCTION

The vascular system is responsible for providing cells with nutrients and oxygen, as well as disposing of their metabolic waste. Without proper vascularization, tissue growth is limited by the oxygen diffusion through tissues (about 200 μm), making new blood vessels essential for tissues to grow beyond smaller size scales.[1] Answering this requirement in a consistent and predictable manner still constitutes an important challenge in tissue engineering (TE). Although there is a tendency for the host to spontaneously create a blood vessel network, the process is often too slow, compromising TE graft integration and survival.[2] Different strategies have been explored to induce angiogenesis based on scaffold microfabrication and functionalization, delivery of angiogenic factors and/or endothelial cells (ECs), and development of bioreactors.[3,4] Nevertheless, there is no convincing evidence that any of these strategies is sufficient to overcome the challenge of adequately vascularize large TE constructs.[5]

Extracellular matrix (ECM) macromolecules such as hyaluronic acid (HA) are important intermediaries of angiogenesis.[6] HA is one of the main structural components of the ECM in its native form (10^6−10^7 Da)[7] but variations in (HA) chain length have been pointed to mediate key steps in angiogenesis.[8,9] Low molecular weight (LMW) HA, produced by the cleavage of the HA molecules during ECM remodeling, was shown to interact with the CD44 receptor and the receptor for hyaluronan mediated motility (RHAMM) promoting ECs proliferation, migration, and sprouting in both *in vitro* and *in vivo* assays.[10,11] Despite the growing evidence on the HA role in vascularization and angiogenesis, its advantage as angiogenic cue in TE constructs is still controversial.[12]

Hydrogels are one of the most common and successful platforms used for TE approaches due to their versatility and high water content. Gelatin methacrylate (GelMA) hydrogels in particular are widely used for their interesting and tunable biological and physical properties. In fact, as it is produced by partial hydrolysis of collagen, the major protein component of the ECM, gelatin carries some of its properties such as cell attaching motifs and metalloproteinase (MMP) cutting sites,

Received: March 10, 2021
Accepted: May 27, 2021
Published: July 16, 2021

https://doi.org/10.1021/acsabm.1c00291
ACS Appl. Bio Mater. 2021, 4, 6023−6035

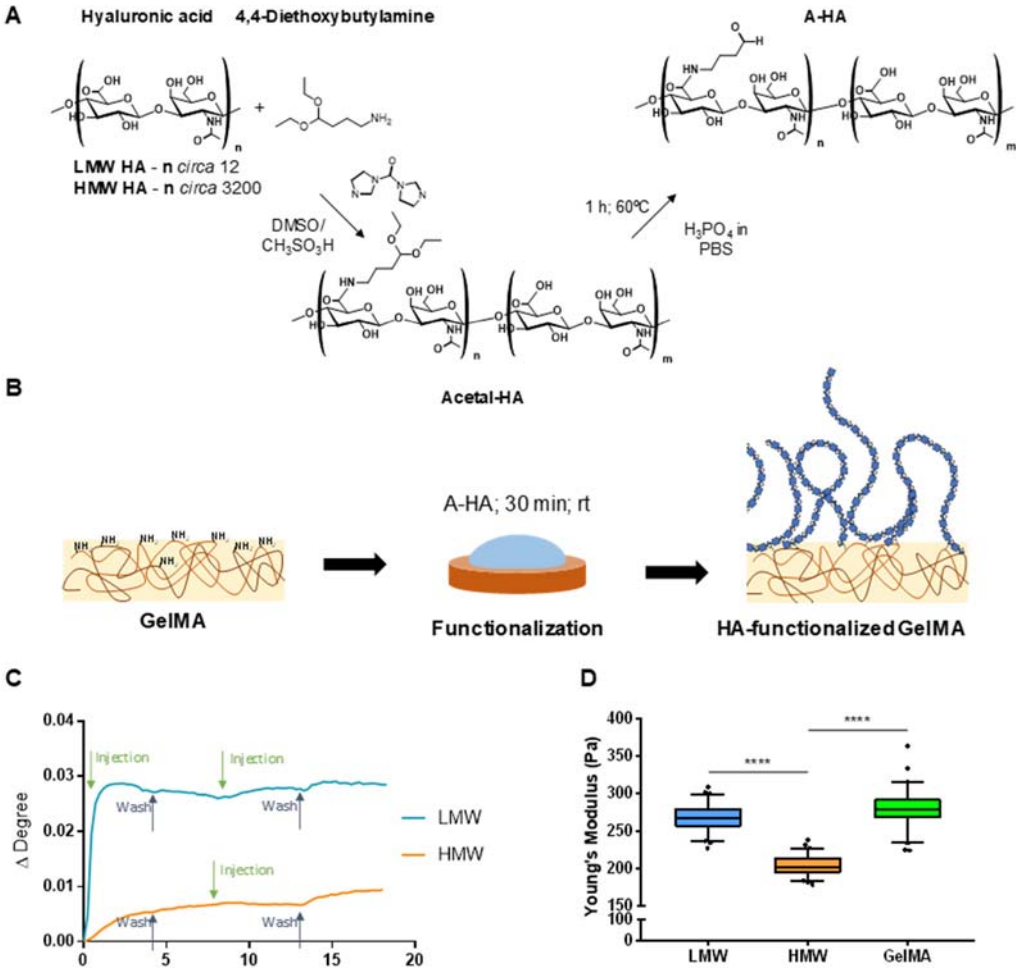

Figure 1. Amine-rich surfaces HA-functionalization. (A) Chemical modification of hyaluronic acid with diethylacetal moieties and acidic deprotection of the aldehydes. (B) Schematics of the protocol used to conjugate A-HA over the amine rich GelMA hydrogels surfaces. (C) SPR analysis of A-HA immobilization on amine functionalized substrates. A volume of 100 μL of 0.005 mg/mL A-HA (LMW and HMW) solution was injected, followed by 5 min of dissociation (wash) with PBS (two injection cycles). Analysis performed at 630 nm, with a constant flow rate of 30 μL/min. (D) Stiffness of the A-HA conjugated 5% w/v GelMA hydrogels. The vertical bars represent the 5−95% confidence interval of, at least, 176 measurements. Statistical differences: ****$p < 0.0001$.

but presenting higher solubility and lower antigenicity than the native collagen.[13,14]

Here we propose a strategy in which immobilization of HA on the surface of gelatin hydrogels is explored as a potential vascularization inducing cue. HA can be used as a surface cue by modifying it with functional groups, such as aldehydes, to create a reactive HA that can be linked to other materials. Several methods of polysaccharides aldehylation, namely the periodate[15] or TEMPO-mediated[16] oxidations create unspecific oxidation and excessive depolymerization of the HA polymeric chain. Herein we explored the introduction of protected aldehydes in the form of an acetal. The mild reaction conditions and amide coupling reagents used to introduce the acetal moieties should prevent the extensive hydrolysis of HA polymeric chain.[17] This allows one to control the molecular weight of the aldehyde-functionalized HA (A-HA), thus enabling the anchorage of HA fragments of low and high molecular weight, to amine functionalized substrates by Schiff's base reaction between A-HA aldehyde moieties and gelatin amine groups.[13,17] The influence of both LMW and HMW HA on ECs behavior was evaluated in terms of viability and proliferation. The expression of angiogenic markers and HA receptors was assessed to explore the vascular oriented responses of HUVECs seeded on the HA modified surfaces. Additionally, the morphological organization, migration and intercellular communication in substrates functionalized with HA of different molecular weights was assessed exploring coculture systems of HUVECs and human dental pulp cells (hDPCs). These approaches will contribute to the understanding of the role of HA molecular weight triggering angiogenesis and its relevance as a biochemical cue for endothelization of TE constructs.

2. MATERIALS AND METHODS

2.1. Preparation of Photo-cross-linkable GelMA Hydrogels. Methacrylated gelatin (GelMA) was synthesized by reaction of gelatin (from porcine skin, Sigma-Aldrich, U.S.A.) with methacrylic anhydride (94%, Sigma-Aldrich, Germany), following previously established protocols[18] (see Supporting Information, SI, for more details). GelMA (5% w/v) was dissolved in PBS containing the photoinitiator 2-hydroxy-4′-(2-hydroxyethoxy)-2-methylpropiophenone (Irgacure 2959; 0.5 wt/v %; Sigma-Aldrich, U.S.A.) to produce a photo-cross-linkable solution and filtered using a syringe/0.22 μm filter system. Then, 80 μL of GelMA solution were put into a PDMS mold (10 mm diameter; 1 mm height) and covered with coverslips. All samples were exposed to UV light, for 50 s using an UV Cross-linker (UV-KUB 2,

https://doi.org/10.1021/acsabm.1c00291
ACS Appl. Bio Mater. 2021, 4, 6023−6035

Kloé, or Omnicure series 2000 EXFO S2000-XLA) at 100% intensity. All these procedures were performed under aseptic conditions.

2.2. Synthesis of Acetal-Hyaluronic Acid (Acetal-HA). Both high molecular weight (HMW;1.5−1.8 MDa HA, Sigma-Aldrich) and low molecular weight (LMW; < 10 kDa HA, Lifecore) HA were functionalized with diethyl acetal moieties (Figure 1A), as described by Mero and co-workers[17] (see SI for more details)

2.3. Determination of Degree of Modification. Nuclear magnetic resonance (NMR) spectroscopy was used to quantify the functionalization of both GelMA and acetal-HA. Samples were prepared by dissolving 5 mg of each material in 1 mL of deuterated water. The ^{1}H NMR spectra were acquired at a frequency of 400.13 MHz at 25 °C with a Bruker Avance III 400. The degrees of functionalization were determined by the ratio of the relative integration of the peaks of the functionalization groups and reference moieties in the starting molecules, as previously described[18] (see SI Figure S2).

2.4. Gel Permeation Chromatography. GPC measurements were performed with a Malvern Viscotek TDA 305 with refractometer (RI-Detector 8110, Bischoff), right angle light scattering (LS) and viscometer detectors on a set of four columns: precolumn Suprema, 5 μm, 8 × 50, Suprema 30 Å, 5 μm, 8 × 300, Suprema 1000 Å, 5 μm 8 × 300 and Suprema Ultrahigh, 10 μm, 8 × 300. The system was kept at 30 °C. PBS with additional 0.05% w/v of NaN_3 was used as eluent at rate of 1 mL min^{-1}. The absolute molecular weight was determined by a calibration of the RI and LS detectors performed using the software Omnisec 4.6.1 (ViskoteK) with a pullulan of M_n 47.1 kDa and PDI 1.09.

2.5. Surface Plasmon Resonance. Surface Plasmon Resonance (SPR) was used for the evaluation of the A-HA immobilization success and rate. Cysteamine coated gold sensors were mounted in SPR (SPR Navi 200, Bionavis) in a Kretschmann configuration. Two 100 μL injections of 0.05 mg/mL solutions of both high and low molecular weight A-HA were performed, followed each injection by 6 min of wash. The analysis was performed to a wavelength of 670 nm at a constant flow of 100 μL/min using PBS as eluent. The resulting curves were used to extract the time at which the reaction was fully completed.

2.6. Hydrogel Functionalization. Acetal-HA batches were subjected to acidic deprotection in order to obtain the aldehyde functional groups, as in Mero et al.,[17] just before needed (Figure 1A; for more details see SI). The functionalization process consisted on the deposition of 100 μL of 0.098 mg/mL HMW or LMW aldehyde-functionalized HA (A-HA) solutions on top of the hydrogel, allowing the reaction for 30 min at room temperature (Figure 1B). The concentration of the HA functionalization solution was previously optimized by *in vitro* assays (see SI). Then, the samples were thoroughly washed with PBS. All procedures were done in sterile conditions.

2.7. Evaluation of the Mechanical Properties. Atomic force microscopy (AFM) analysis was carried out on A-HA functionalized GelMA surfaces with HMW A-HA, LMW A-HA, or plain. Hydrogels were produced according to the procedure described in the points above. Tests were carried using a JPK NanoWizard 3 (JPK Instruments, Germany) with qp-BioAC−CB2 probes (nominal $k \approx 0.1$ N/m, Nanosensors, Switzerland), calibrated using the contact-based method to determine the sensitivity and k. Each sample was mounted under a hydrated medium (PBS, at room temperature) and 8 × 8 maps were recorded using square acquisition frames of 10 × 10 μm. For each sample, 3 force maps were collected in different positions on the surface. The Young's modulus was retrieved from each individual force curve, at least 55 per force map, by fitting with the Hertz/Sneddon model using the JPK SPM Data Processing software (JPK Instruments, Germany).

2.8. Cell Culture and Expansion. Human Umbilical Vein Endothelial Cells (HUVECs) were expanded in polystyrene tissue culture flasks coated with 0.7% w/v gelatin (gelatin from porcine skin, Type A, Sigma-Aldrich, U.S.A.) solution, previously autoclaved. Cells were cultured with endothelial cell basal media (Millipore S.A.S, France) supplemented as by manufacturer's instruction. Human Dental Pulp Cells (hDPCs) were obtained from available cryopreserved stock populations isolated from human third molars under the scope of previous studies.[19] The hDPCs were cultured with Dulbecco's Modified Eagle's Medium—low glucose (DMEM, Sigma-Aldrich, U.S.A.) with 10% fetal bovine serum (FBS, Life Technologies, U.S.A.) and 1% antibiotic/antimycotic as supplements. The cells were incubated at 37 °C in a 5% CO_2 humidity-saturated atmosphere, and the culture medium renewed each 2−3 days. HUVECs and hDPCs at passage 5 were used for these studies.

2.9. In Vitro HUVECs Response to HA-Functionalized GelMA Hydrogels. After production of HA-functionalized hydrogels, expanded HUVECs were trypsinized, counted and seeded onto the surface of the hydrogels in a cell density of 2.5 × 10^4 cells/cm^2. A droplet of 100 μL of 2 × 10^5 cells/mL cell suspension was placed onto each hydrogel and incubated for 4 h to enhance cell adhesion. Then, culture media was added to a total of 500 μL per well/sample. Plates were incubated at 37 °C for 1, 3, and 7 days with medium replacements every 2−3 days.

At least 3 samples from each formulation were used for the assays.

2.9.1. Metabolic Activity Assessment. Cell metabolic activity was assessed by means of the AlamarBlue (Biorad, U.K.) assay, according to manufacturer's recommendations. First, a 1:10 v/v solution of AlamarBlue in endothelial cell medium was produced. The culture medium was removed from each sample and replaced with a volume of 500 μL of the solution. Samples were then incubated for 3 h at 37 °C and protected from the light. After, 100 μL of each sample were collected in triplicate to a 96-well plate and the fluorescence measured with a microplate reader (Infinite M200Pro, Tecan, Switzerland; Synergy HT, Bio-Tek Instruments, U.S.A.) at excitation and emission wavelength of 530 and 590 nm, respectively.

2.9.2. Cell Proliferation. Cell proliferation was evaluated as a function of the total amount of double-stranded DNA present at different culture times (1, 3, and 7 days), using the Quant-IT PicoGreen dsDNA Assay Kit (Thermofisher, U.S.A.). Samples were washed with PBS and collected with 1 mL of ultrapure water. After incubation at 37 °C for 1 h, samples were frozen at −80 °C for at least 2 h or until further testing, for which the manufacture's recommended procedure was followed.

2.9.3. Immunocytochemistry. At the end of each time point, hydrogels were fixed with 10% (v/v) formalin for 45 min at room temperature. After permeabilization for 1 h with 0.1% (v/v) Triton X-100 (Sigma-Aldrich, U.S.A.) in PBS, under agitation and at room temperature, samples were rinsed with PBS (3 times) and stained with a conjugated antibody. Samples were incubated with CD31 (Allophycocyanin/APC conjugated mouse monoclonal Anti-Human CD31/PECAM-1, R&D Systems, U.S.A.), CD44 (PE Mouse Anti-Human CD44, BD Pharmingen, U.S.A.) or pERK1/2 (Mouse monoclonal to ERK1 + ERK2 (phospho T185 + Y187 + T202 + Y204), Abcam, U.K.) antibodies diluted in 0.1% Bovine Serum Albumin (BSA; Sigma-Aldrich, U.S.A.) in PBS overnight at −4 °C and under agitation. Nuclei and cytoskeleton were counterstained with DAPI 1:1000 v/v (Biotium, U.S.A.) and phalloidin 1:500 v/v for 30 min at room temperature, under agitation. The samples were again washed with PBS 3 times. Samples were acquired by confocal laser scanning microscopy (CLSM, Leica TCS SP8, Microsystems, Wetzlar, Germany). Images were bidirection scanned at 400 Hz with UV (405 nm) and visible lasers (488 nm Argon, 561 and 633 nm HeNe), and data processed using LAS X software from Leica.

2.9.4. Assessment of Metalloproteinases Activity. The presence of metalloproteinases in culture medium correspondent to each condition was analyzed by zymography, according to the protocol of Ren et al.[20] (for more details, see SI). Each sample was mixed with Laemmli sample buffer (1:1 ratio) and left at room temperature for 30 min. Samples were subjected to SDS-Page using a 10% SDS-polyacrylamide gel containing 4 mg/mL of gelatin (Sigma-Aldrich, U.S.A.). Gels were run in a vertical electrophoresis apparatus (Miniprotean 3, BioRad, U.S.A.) at a constant voltage of 125 V for approximately 2 h. Then, gels were removed and incubated in renaturing buffer (2.5% Triton X-100) for 30 min under gentle agitation. Afterward, gels were incubated in developing buffer (50 mM Tris-Base; 0.2 M NaCl; 5 mM $CaCl_2$) and left under gentle shaking for 30 min at room temperature, followed by incubation with fresh developing buffer for 18 h at 37 °C. Staining solution (0.5% Comassie blue R-250; 25% isopropanol; 10% acetic

https://doi.org/10.1021/acsabm.1c00291
ACS Appl. Bio Mater. 2021, 4, 6023−6035

Table 1. List of primers used for the rt-PCR analysis

NCBI reference sequence	gene product	gene short name	primer sequence	product length [bp]
NM_000610.3	cluster of differentiation 44	CD44	CAGCACCATTTCAACCACACC	147
			GCAGTGGTGCCATTTCTGTCT	
NM_001142556.1	receptor for hyaluronic acid mediated motility	RHAMM	AAAGATGAGGGGTATGATGGCT	72
			TCGAGACTCCTTTGGGTGAC	
NM_001795.4	cadherin-5	CADH5	ATGAGATCGTGGTGGAAGCG	125
			TGTGTACTTGGTCTGGGTGAAG	
NM_002253.3	vascular endothelial growth factor receptor -2	KDR	GAGGGGAACTGAAGACAGGC	144
			GGCCAAGAGGCTTACCTAGC	
NM_001256799.1	glyceraldehyde-3-phosphate dehydrogenase	GAPDH	GGGAGCCAAAAGGGTCATCA	198
			GCATGGACTGTGGTCATGAGT	

Table 2. GPC Analysis Results for HMW and LMW HA, in Unmodified, Acetal Functionalized, and Aldehyde Activated States[a]

sample	M_n (kDa)	M_w (kDa)	PDI	elution volume (RI/LS)
HA HMW (unmodified)	447[b]	463[b]	1.03	18.61/18.51
Acetal-HA HMW	234[b]	287[b]	1.22	20.16/19.71
A-HA HMW	212[b]	260[b]	1.22	20.47/19.91
HA LMW (unmodified)	2.3	3.9	1.60	25.5
Acetal-HA LMW	17[c]	123[c]	7.29	25.5/21.29
A-HA LMW	27.3[c]	122[c]	4.48	23.23/20.37

[a]M_n represents the number average molecular weight, M_w the weight average molecular weight and PDI the polydispersity index (M_w/M_n). [b]Underestimation of the M_w by light scattering at 90 deg occurs. [c]Overestimation due to aggregation due to hydrophobicity.

acid) was used for 30 min to stain the gel, followed by treatment with destaining solution (methanol, acetic acid, H_2O in a 50:10:40 proportion) until bands were clear and sharp.

2.9.5. Evaluation of Gene Expression through Real Time Polymerase Chain Reaction (rtPCR). After 1, 3, and 7 days in culture, samples were collected in TRI reagent (Sigma-Aldrich, U.S.A.) and stored at −80 °C, until RNA isolation according to manufacturer's procedure. The yield and purity of RNA isolation was determined by spectrometry using the NanoDrop 1000 Spectrophotometer (Thermo-Scientific). The cDNA was synthesized using 100 pg of RNA as template and the qScript cDNA Synthesis Kit (Quanta BioSciences). Primers were designed using the primer-BLAST tool available at http://www.ncbi.nlm.nih.gov/tools/primer-blast. To avoid the amplification of genomic DNA or pre-RNA (nonspliced RNA), the primers were designed in order to span the exon−exon junctions. Target genes listed in Table 1 were normalized to the reference housekeeping *GAPDH* gene expression in HUVECs before seeding (day 0). The analysis was performed on an RT-PCR Mastercycler (Realplex, Eppendorf).

2.10. Assessment of Endothelial Cell Ingrowth into Mesenchymal Cells-Laden Constructs. In order to test the system's ability to prolong viability of encapsulated cells, a coculture system was developed combining hDPCs encapsulated in the GelMA hydrogels and HUVECs seeded on top of the hydrogel. For that, hDPCs were resuspended in a sterilized GelMA solution of 5% w/v at a concentration of 4×10^6 cells/mL. Hydrogels encapsulating hDPCs were then conjugated with the A-HA precursors following the same method as the simple hydrogels, and HUVECs were seeded on top of the functionalized surfaces as above-described. The constructs were cultured in endothelial cell basal media, renewed every 2−3 days, for 1, 3, and 7 days.

HUVECs' ingrowth was evaluated by confocal microscopy, after staining with CD31 and CD44, as described above.

2.11. Evaluation of Angiogenic and Antiangiogenic Proteins Presence in Conditioned Medium. The relative expression of 55 different angiogenic and antiangiogenic proteins in the coculture systems was quantified in conditioned medium collected after 7 days of culture, by Human Angiogenesis Antibody Array kit (Proteome profiler; R&D Systems, Minneapolis, MN, U.S.A.) (more details in the SI).

The imaging was performed in a LICOR Odissey FC system (LICOR, Spain). The mean dot pixel intensity was measured using the "Microarray_profile" plugin of the public domain FIJI software (NIH).

2.12. Statistical Analysis. Statistical analysis was conducted through the software GraphPad PRISM 8.0. (GraphPad Software Inc., San Diego, CA, U.S.A.) by one-way or two-way analyses of variance (ANOVA), after excluding outliers (iterative Grubb's method) and testing the normality (Kolmogorov−Smirnov test). A level of significance of $p < 0.05$ (minimum of 95% confidence interval) was considered to appoint conditions as statistically significant. Statistically significant values of interest are annotated in their respective graphs.

3. RESULTS

3.1. Material Synthesis and Characterization. *3.1.1. Modification Degree and Impact on Molecular Weight Maintenance.* The introduction of the acetal groups in both LMW and HMW HA was confirmed by FTIR and ^{1}H NMR analysis (Figures S1 and S2). Degrees of modification (defined as the percentage of modified disaccharide units) of 12 ± 3%, and 5 ± 2% were determined for the LMW HA and the HMW HA, respectively. A degree of methacrylation of 54 ± 2% was calculated for GelMA by ^{1}H NMR analysis. The molecular weight of the HA precursors, before and after functionalization (Acetal-HA), and after aldehyde deprotection (A-HA), was evaluated by gel permeation chromatography (GPC) with a refractive index and a light scattering (LS) detector at 90°. The results, summarized in Table 2, indicate that the functionalization process did partially break down the polymer both during the introduction of the acetal and deprotection steps. The higher degree of modification of LMW HA induces aggregation, as observed in the LS detector (see SI Figure S3). Hence, the apparent molecular weight and PDI of both acetal-HA and A-HA are higher than the starting material. In any case, the GPC analysis shows that the molecular weight of the HMW A-HA is within the high molecular weight range and the LMW A-HA in the low molecular weight range. In this sense the chemistry selected serves for the purpose of comparing the angiogenicity vs

https://doi.org/10.1021/acsabm.1c00291
ACS Appl. Bio Mater. 2021, 4, 6023−6035

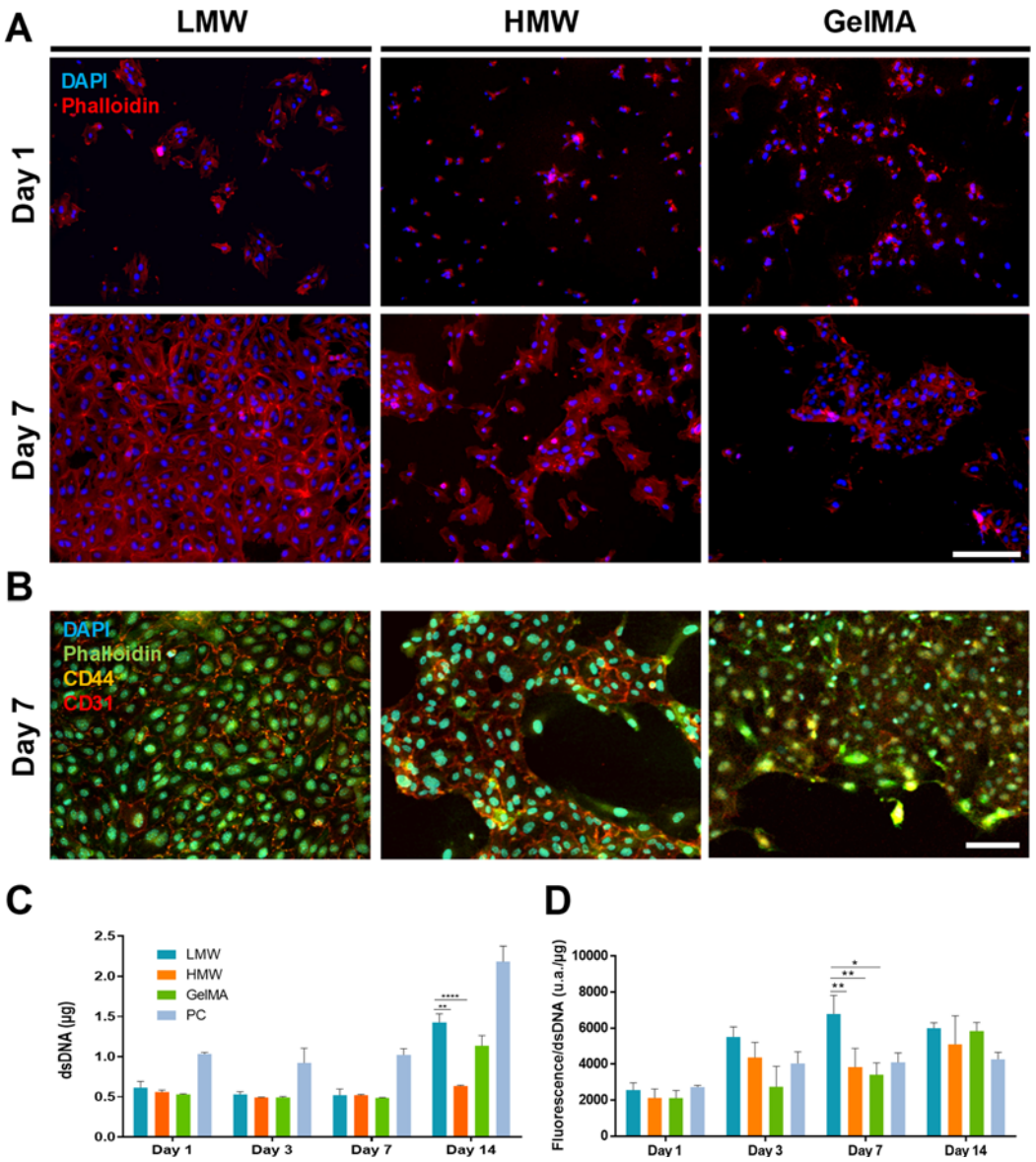

Figure 2. (A) DAPI (blue) and phaloidin (red) stained micrographs of HUVECs seeded onto GelMA hydrogels functionalized with A-HA formulations of LMW, HMW, or plain GelMA, cultured for 1, 3, 7, and 14 days. Scale bar measures 200 μm. (B) Confocal micrographs of HUVECs at day 7 stained with DAPI (blue) phalloidin (green) and immunolabeled samples with CD44 (yellow) and CD31 (red). Scale bar measures 100 μm. (C) dsDNA quantification and (D) metabolic activity normalized to dsDNA content for HUVECs seeded onto GelMA hydrogels, plain or functionalized with HMW or LMW A-HA, after 1, 3, 7, and 14 days. Tissue culture polystyrene was used as positive control (PC); $N = 3$. Statistical differences are represented in the graph for relevant parameters, with $^{*}p < 0.05$, $^{**}p < 0.01$, $^{****}p < 0.0001$.

high/low molecular weight HA. Additional details on GPC analysis are presented in the SI.

3.2. Assessment of HA Surface Immobilization. The success of the A-HA immobilization over amine-presenting surfaces was assessed by surface plasmon resonance (SPR) (Figure 1C). SPR curves confirmed that both LMW and HMW A-HA immobilized onto the amine functionalized surface, with a notable difference between the immobilization speed. For both LMW A-HA and HMW A-HA the surface saturation was almost reached after the first injection cycle (100 μL of 0.05 ng/mL). Moreover, the bonding to the amine surface was irreversible as observed by the nondissociation of the immobilized HA after the PBS washes. It was also observed that a higher mass of LMW A-HA was bound to the surface than HMW A-HA.

The effect of HA conjugation on the surface mechanical properties of GelMA hydrogels was assessed by atomic force microscopy (AFM). The surface Young's modulus obtained for hydrated samples (Figure 1D) suggests that A-HA functionalization decreased the overall stiffness of GelMA hydrogels. GelMA hydrogels present a Young's modulus of 278.5 ± 36.1 Pa and become softer as the molecular weight of A-HA increases (268.4 ± 4.6 Pa and 204.5 ± 6.8 Pa for LMW and HMW, respectively) ($p < 0.0001$).

3.3. In Vitro Evaluation of Human Umbilical Vein Endothelial Cells (HUVECs) Response to the HA Functionalization. *3.3.1. HUVEC Morphology, Viability, and Proliferation.* In order to assess the cell response to the modified surfaces, HUVECs were seeded on top of GelMA hydrogels or hydrogels functionalized with HMW A-HA or LMW A-HA. Cell culture plastic surfaces were used as controls.

At day 1, HUVECs presented a rounded shape which is consistent with their early stage of adherence. For the

https://doi.org/10.1021/acsabm.1c00291
ACS Appl. Bio Mater. 2021, 4, 6023−6035

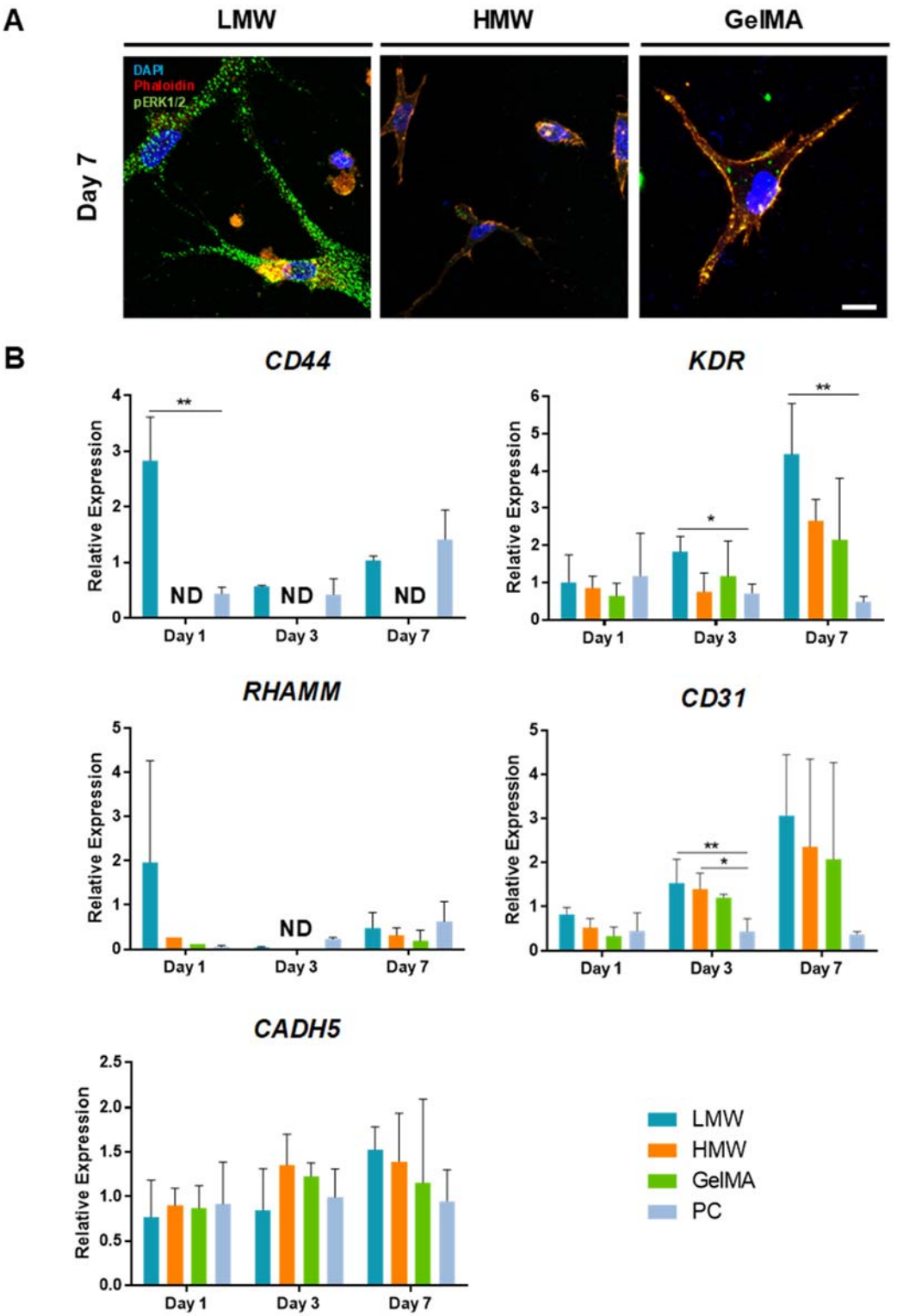

Figure 3. (A) Representative micrographs of phosphorilated ERK1/2 in HUVECs seeded onto LMW, HMW, and GelMA, after 7 days in culture. (B) Gene expression analysis of HA binding and angiogenesis related markers CD44, KDR, CADH5, CD31, and RHAMM after 1,3 and 7 days of culture, with data presented for the LMW, HMW, GelMA, and Positive Control (PC) conditions. Normalization was performed to GAPDH expression in trypsinized HUVECs before seeding. ND (None detected) represents time points for which no template was amplified for a specific formulation. Statistical differences are represented in the graphs as $*p < 0.05$ and $**p < 0.01$.

subsequent time points, cells showcased a more cobblestone shape, characteristic of these ECs. Interestingly, the LMW A-HA hydrogels generally present more cell clusters than their counterparts (Figure 2A and 2B).

Cell metabolic activity and proliferation were also evaluated. As depicted in Figure 2D, metabolic activity per cell increased for all formulations over time, but was higher in LMW than in the HMW and plain GelMA hydrogels at day 7. The evolution of

https://doi.org/10.1021/acsabm.1c00291
ACS Appl. Bio Mater. 2021, 4, 6023−6035

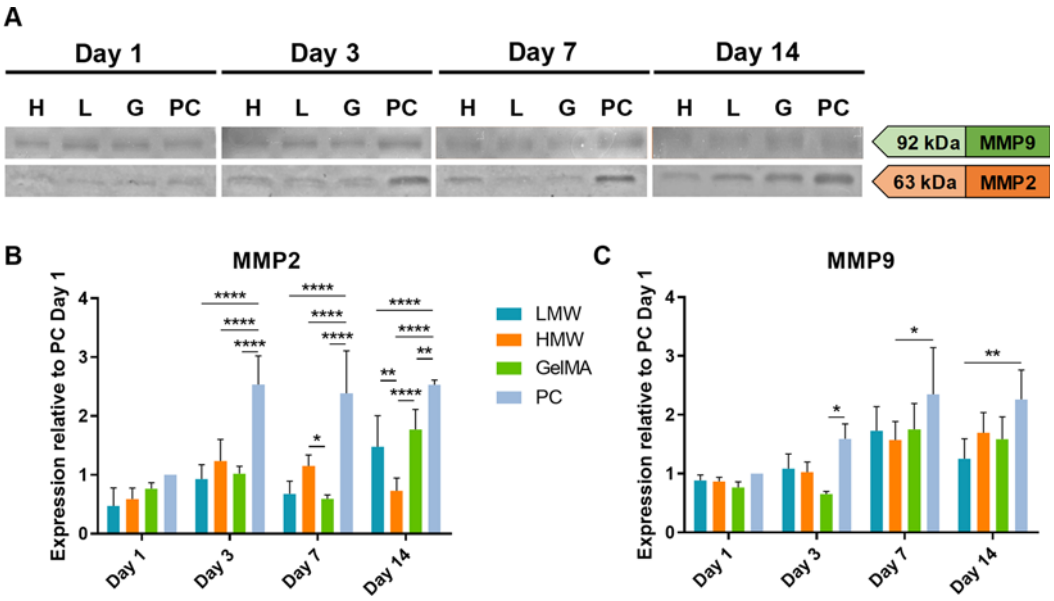

Figure 4. Expression of metalloproteinases. (A) Zymogram of conditioned media collected at 1, 3, 7, and 14 days of culture of HUVECs on HMW HA (H), LMW HA (L), GelMA (G), and polystyrene (PC). MMP-9 and MMP-2 positions are indicated. Relative expression of (B) MMP-2 and (C) MMP-9, normalized to the expression in PC at day 1. Statistical differences are represented in the graph with *$p < 0.05$; **$p < 0.01$ and ****$p < 0.0001$.

cell proliferation (Figure 2C) during the first 7 days seems similar for all conditions, characterized by a lower cell content in all formulations, compared with the positive control, suggesting impaired initial adhesion to the GelMA and A-HA functionalized surfaces. However, at day 14, cell proliferation is increased in the LMW A-HA surfaces with significant differences in comparison with the HMW A-HA ($p < 0.01$) and with the plain GelMA hydrogel ($p < 0.0001$).

3.3.2. HA-Mediated Phenotypic Response. To investigate the HA-CD44 downstream signaling, the ERK1/2 pathway activation was investigated (Figure 3A). It was observed a strong phosphorylation of ERK1/2 in HUVECs growing in LMW HA while almost no signal was detected for HMW HA and GelMA formulations.

Figure 3B presents the results of the real time Polymerase Chain Reaction (rtPCR) analysis conducted for *CD44*, *CD31*, *KDR*, *RHAMM*, and *CADH5* genes. The *CD44* was overexpressed after 1 day in cells cultured on LMW A-HA functionalized surfaces, returning to basal levels for increasing culture times. Comparatively, the culture on polystyrene coverslips in standard culture conditions (positive control; PC) maintained a stable basal expression. Remarkably, no *CD44* expression was detected in the HMW A-HA and GelMA hydrogel formulations. A similar trend was observed for *RHAMM*. *CD31* expression increased in LMW and HMW A-HA conditions in comparison to the PC at day 3 ($p < 0.05$). *CADH5* expression was unchanged regardless of the condition, while the *KDR* expression increased in cells cultured on the LMW A-HA hydrogels at day 3 and day 7.

The presence of important metalloproteinases for the initial steps of angiogenesis, MMP-2 and MMP-9, was analyzed by zymopgraphy (Figure 4) in the conditioned media of HUVECs cultured over the tested formulations up to 14 days (see SI Figure S7). MMP-2 expression in HMW A-HA functionalized surfaces peaks around day 7 ($p < 0.05$), while in GelMA and LMW A-HA formulations tended to increase up to14 days in culture (Figure 4B). Regarding MMP-9 expression, it tended to increase in all conditions beyond day 3, except for the LMW A-HA, which showed a reduced expression after day 7 ($p < 0.05$) (Figure 4C).

3.4. Assessment of the A-HA Functionalization Effect in ECs Migration. CD31 and CD44 positive cells were detected and analyzed on the surface of the hydrogels (Figure 5B). Side profiles enabled to visualize the infiltration of HUVECs into the hydrogels (Figure 5C,D) and the migratory distance was determined through a color quantification vs surface distance plot. Results show that HUVEC ($CD31^+$ cells) infiltrate into the LMW A-HA hydrogel up to 200 μm in depth, which was the maximum thickness of hydrogel herein analyzed. For the other two conditions the maximum infiltration distance was around 60 μm. As well, the highest level of diffusion for $CD44^+$ cells was observed in the LMW A-HA conditions.

3.5. Angiogenic Protein Profile of Cocultures Conditioned Medium. Twenty angiogenic and antiangiogenic proteins were identified in the conditioned media of hDPCs/HUVECs cocultured in the different hydrogels' formulations (Figure 6). The A-HA functionalization strongly favor the expression of amphiregulin (AREG), hepatocyte growth factor (HGF), insulin-like growth factor-binding protein (IBP)-2 and -3, pigment epithelium-derived factor (PEDF), metalloproteinase inhibitor-1 (TIMP-1), and vascular endothelial growth factor (VEGF). However, baseline signals of endoglin (ENG) are only detected in cells laden in GelMA formulation (see SI Figure S8), which also seems to favor the expression of endothelin-1 (EDN1). Remarkably, the endostatin/collagen XVIII (COLXVIII) is expressed in all the conditions except in the LMW A-HA hydrogels.

4. DISCUSSION

This study aimed to explore the use of HA of different molecular weights as a vascular trigger for TE constructs vascularization. In order to nourish the tissue substitute and enable connection to the vasculature of the patient, new vascular-like structures are to be formed from a cascade of events, starting with the increase of vascular permeability, to the degradation of the ECM and culminating in the proliferation, migration, and organization of

https://doi.org/10.1021/acsabm.1c00291
ACS Appl. Bio Mater. 2021, 4, 6023−6035

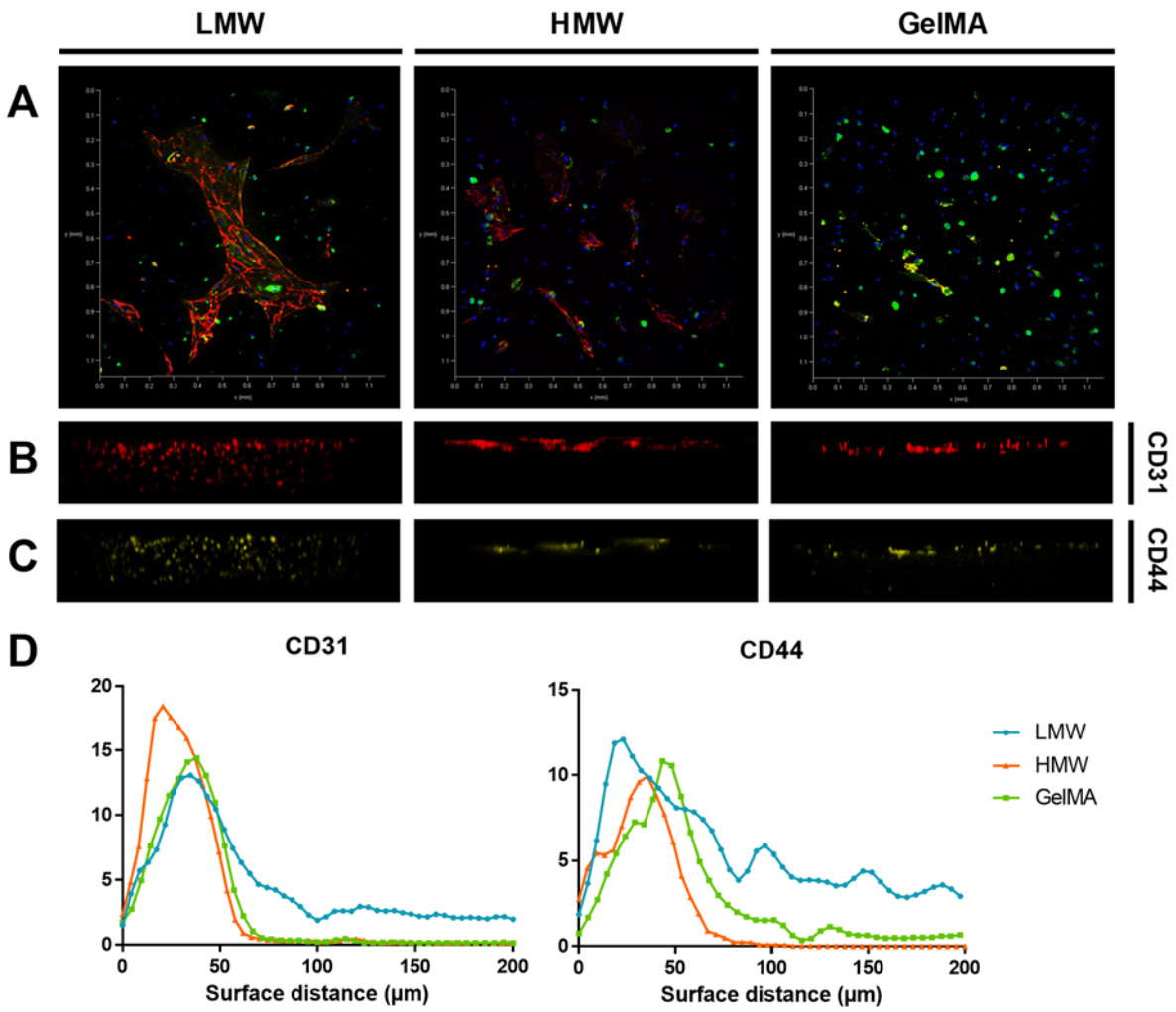

Figure 5. (A) Representative three-dimensional projections of the hydrogels with cocultures of hDPCs and HUVECs after 7 days in culture. Surface view of the cell laden hydrogels immunolabeled with CD44 (yellow) and CD31 (red) and counterstained with DAPI (blue) and phalloidin (green). Side view projections of the cell-laden hydrogels, showing the distribution of (B) CD31 and (C) CD44 positive labeling. (D) Color quantification of cell markers as a function of the distance to the sample surface.

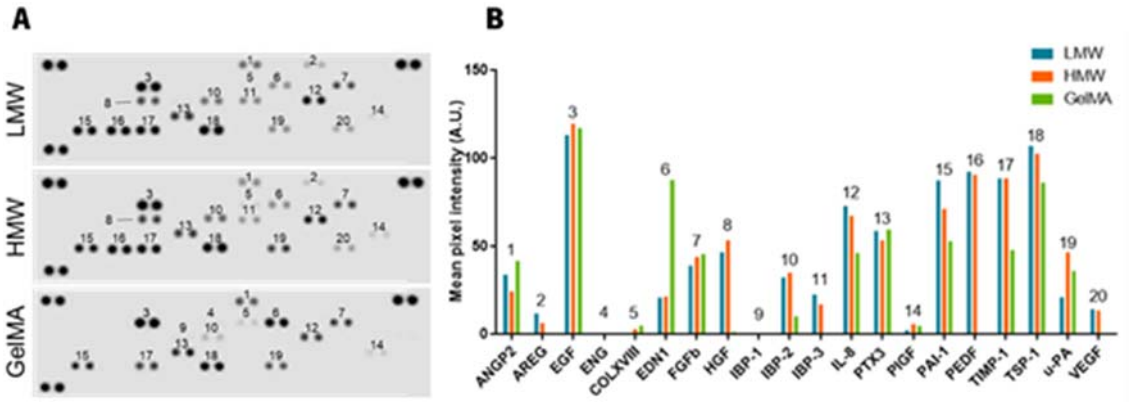

Figure 6. Angiogenic and antiangiogenic proteins profile in conditioned medium obtained from hDPCs/HUVECs cocultures at day 7. (A) Proteins detected by the human angiogenesis antibody array in the conditioned medium of cocultures cultured in hydrogels functionalized with LMW A-HA, HMW A-HA, or plain (GelMA). (B) Histogram of mean pixel density in each spot. Numbers above each column set represent the protein spotted on the membrane showed in (A).

ECs.[21,22] The ability to control or influence this mechanism is critical for the success of generating functional tissue/organs substitutes in TE applications.

LMW HA exogenous supplementation has been reported to have a positive effect on attachment and proliferation of tumorigenic or sound cell lines, conversely to HMW HA supplementation.[12,23,24] This response depends on the specific

https://doi.org/10.1021/acsabm.1c00291
ACS Appl. Bio Mater. 2021, 4, 6023−6035

interaction of HA with cell receptors, such as CD44. While HMW HA binds to the extracellular domain of HA binding proteins in a polyvalent manner inducing CD44 clustering,[23] HA oligomers interact with cell receptors in a monovalent manner competing with native HA for CD44 binding, and inhibiting CD44 clustering[23] thus contributing to the onset of distinct CD44 signaling pathways. While the HMW HA-CD44 interaction is anti-inflammatory and antiangiogenic; LMW HA-CD44 (4−25 disaccharide units) is proangiogenic and stimulate the expression of pro-inflammatory cytokines, chemokines, and growth factors.[25,26] However, the effects of HA molecular weight in triggering the angiogenesis of TE constructs are controversial. In a recent study, Sapudom and co-workers reported that only soluble LMW-HA promotes cell proliferation in a CD44 dependent manner unlike HMW-HA and LMW-HA immobilized onto fibrillary collagen I scaffolds by 1-ethyl-3-(3-(dimethylamino)propyl) carbodiimide (EDC) cross-linking.[12] Both the carboxylate oxygens of GlcUA7 and N-acetyl group of GlcNAc6 from HA disaccharide are important for CD44-HA binding.[27] Moreover, the minimum effective unit for HA to CD44 binding was determined to be a 6-mer; however, 8- to 12-mers are more efficient competitors. Therefore, the extensive HA modification by EDC cross-linking thought the carboxyl groups,[12] or methacrylation of the GlcNAc6 C6 primary alcohol,[28,29] impairs CD44-HA signaling.

Here, HA ligands were developed by inserting aldehyde groups into the HA chain, allowing its association with amine-functionalized surfaces through Schiff-base reaction.[30] The reaction of aldehydation by the acidic deprotection of acetal protected aldehydes was chosen to overcome the over-break-down or over-modification issues of the HA molecular chain associated with other reported methods[16,31] In our system, the controlled degree of modification of 12% of the disaccharides of the 20-mers LMW A-HA (i.e., 1.2 disaccharides per molecule in average) generates unmodified ends with, at least, 10-mers after immobilization, which was expected to preserve its physiological activity. Although the process partially breaks down the polymer, GPC results showed the molecular weight range was maintained for both the acetal-HA form and the A-HA after the activation process. The modification degree differences between Acetal-LMW and Acetal-HMW-HA (12 and 5% respectively), are a direct consequence of the steric hindrance of HA molecules, which increases with molecular weight.[32] In addition, for LMW HA a much higher mobility in solution is expected, increasing the probability of the diethyl acetal and HA molecules interact and react.

Gelatin methacrylate hydrogels were chosen as the substrate model for studying the A-HA functionalization, given the wide applications of these hydrogels in TE.[13,14] Moreover, gelatin is rich in amines, from the lysine and hydroxilysine residues,[33] making it ideal for the functionalization here developed.[30] However, despite the GelMA hydrogels possess arginine-glycine-aspartic acid (RGD) motifs for focal adhesion, typical adhesion proteins like fibronectin are still missing inside the bulk hydrogel and need to diffuse from the media into the hydrogel to exert their effects. This effect is reported throughout the literature, for instance by,[34] who showed that the adhesion and overall biologic response of GelMA hydrogels was enhanced by incorporation of the fibrinogen and growth factors-rich human platelet lysate. In particular, the 5% GelMA hydrogels were selected based on the evidence of low HUVECs adhesion and proliferation when seeded onto these hydrogel formulations in previous studies performed by Prof. Ali Kademhosseini group[35].

The immobilization kinetics of the A-HA to amine-rich surfaces was assessed by SPR. Our data confirmed not only that A-HA of low and high MW were able to adhere irreversibly over surfaces presenting reactive amines, but also that they saturate the surface within only a few minutes. LMW HA binding showed itself to be considerably faster than HMW HA and to promote a higher mass deposition than the HMW HA. This can be related both with the degree of modification of the LMW HA which is higher than that of the HMW HA, therefore having a faster reaction with the amines in the surface, and the higher strict hindrance of HMW HA to additional HA molecules to link to the surface, forming thicker but less dense layers.[36,37]

The values of Young's modulus obtained for plain GelMA (278.5 ± 36.1 Pa) and LMW A-HA (268.4 ± 4.6 Pa) hydrogels were in the range of similarly produced hydrogels.[38] However, the linkage of HA with different molecular weights to the surface of GelMA hydrogel influenced the mechanical properties of the hydrogels' surface. As for the HMW A-HA (204.5 ± 6.8 Pa) functionalized surfaces, results showed an overall decrease in Young's modulus compared to GelMA hydrogels ($p < 0.05$). These values were justified by other authors on the high capacity of HA to adsorb and retain water and form swelled layers.[36] The specific differences between LMW and HMW are consistent with other reports, in which the decrease in stiffness is sharper for HMW than for LMW adsorbed surfaces.[37−39] Additionally, the stiffness depends on the cross-linking degree of the polymeric matrices.[40] Therefore, the lower stiffness of the HMW A-HA functionalized hydrogels can also be a direct consequence of its lower modification degree.

Initial HUVECs adhesion and proliferation to the GelMA and HA functionalized hydrogels was impaired, as anticipated.[35] Significant differences in terms of cell number were only observed after 14 days in culture in the LMW-HA functionalized surfaces, suggesting that the physiological role of LMW HA was preserved. LMW HA-CD44 binding initiates tyrosine phosphorylation of Src, FAK, and ERK1/2, upregulating the expression of c-jun and c-fos, thus modulating cell adhesion, proliferation, and motility.[23,41,42] Herein, a strong phosphorylation of ERK1/2 in HUVECs growing in LMW HA was observed (Figure 4A), while almost no signal was detected for HMW HA and GelMA formulations, as previously reported for LMW HA and HMW HA supplementation to HUVECs.[8,23]

The CD44-ERK1/2 activation by LMW HA functionalized surfaces enhanced the expression of the angiogenesis related genes *CD44*, *CD31*, and *KDR* (Figure 4B), and peaked the HUVECs metabolic activity around day 7 (Figure 3A). *CD31/PECAM-1* codes for a trans-membrane protein highly expressed at endothelial cell−cell junctions. It functions as an adhesive stress-response protein which contributes to maintain ECs junctional integrity,[43] as observed in Figure 3C. Moreover, the KDR or VEFR2 is a tyrosine-protein kinase, acting as a cell-surface receptor for VEGFA, and is fundamental in the regulation of angiogenesis, vascular development, vascular permeability, and embryonic hematopoiesis.[44]

MMPs expression was also assessed given their importance in the overall process of angiogenesis, actively remodeling ECM, creating space for ECs to migrate and sprout, and modulating the bioavailability and function of several angiogenic factors namely TGF-β[45] and VEGF.[46,47] Here, we found that MMP-2 and MMP-9 expression along the time in culture is also HA molecular weight dependent. While MMP-2 expression increased only for HUVECs seeded on LMW HA and GelMA substrates, the MMP-9 expression increased sustainably over-

https://doi.org/10.1021/acsabm.1c00291
ACS Appl. Bio Mater. 2021, 4, 6023−6035

time in all the conditions, except for LMW HA functionalized surfaces, in which a lower expression was observed from day 7 on. MMP-2 and MMP-9 have been described to have antagonistic effects in angiogenesis. For instance, in corneal vascularization, MMP-2 activity is higher in neovascularization and mainly localized in ECs infiltrating areas.[48] Conversely, MMP-9 is prominently expressed at the border of regenerating corneal epithelium in areas with epithelial wounding but was not detected in the vascularized stroma,[49] and is involved in the generation of molecular inhibitors of angiogenesis.[49,50]

The angiogenic effect of LMW HA functionalization in a potential TE application was also assessed using a coculture system. Mesenchymal stem cells (MSCs) have the potency to promote angiogenesis via paracrine activity.[51,52] The hDPCs, a MSCs-like cell population isolated from the dental pulp, were described to release the proangiogenic factors; VEGF and HGF.[53] However, when encapsulated into hydrogels or scaffolds, they usually fail to induce vascularization, unless external angiogenic factors are provided.[54] Thus, in this study, we assessed whether potentiating the proangiogenic phenotype in HUVECs, the LMW-HA immobilization would foster the vascularization of TE constructs and promote the paracrine communication between ECs and MSCs, together with the empowerment of the proangiogenic phenotype in HUVECs.

As previously shown by us,[54] hDPCs encapsulated into hydrogels facilitated the ingrowth of the ECs under angiogenic conditions as observed, herein, in the LMW HA functionalized constructs. Actually, other works have reported the facilitation of tube formation and maturation by HUVECs *in vitro* by hDPCs, which act as pericytes.[55]

The analysis of angiogenic and antiangiogenic proteins in the conditioned medium of hDPCs/HUVECs cultured for 7 days showed that HA functionalization induces the release of VEGF, but not in the plain GelMA or HUVECs cultured in standard conditions (SI Figure S8), suggesting a hDPCs origin. VEGF is a major player in angiogenesis. The VEGF-KDR interaction induces a tyrosine kinases signaling pathway that stimulates proliferation, migration, and production of several factors in ECs.[56] The synergistic effect of VEGF and CD44-mediated activation of ERK1/2 may justify the deep infiltration of HUVECs into the LMW HA functionalized hydrogels encapsulated with hDPCs.

Breaking down some of the proteins detected, the presence of ANG-2 is also distinctive in all three formulations. This growth factor is generated by metalloproteinase cleavage, namely MMP-9,[43,49] of the circulating plasminogen. It is a competitor of ANG-1, and, in the absence of angiogenic inducers, such as VEGF, may lead to loosening of ECs-matrix contacts and eventual cell apoptosis. However, when in action with VEGF, it may enable ECs migration and proliferation, serving as an angiogenic signal.[57] As mentioned before, VEGF was only identified in HA functionalized samples, suggesting that the complementary action with ANG-2 may only exist in the presence of HA. AREG expression also seems to be HA dependent. This is a ligand of the EGF receptor and is connected with mitogenic events.[58] HGF is a growth factor secreted by hDPCs[53] that was only expressed in the HA functionalized formulations. It is involved in the transduction of signals from the ECM to the cytoplasm by binding to the HGF ligand. Besides, it regulates processes like proliferation and ECs morphogenesis.[59] IBP-3 release seems to be linked to HA functionalization as well. This protein is one of six high affinity IGF binding proteins, that has been reported to enhance cell motility and inhibiting apoptosis in HUVECs by activation of the sphingosine kinase (SphK) pathway.[60] This activation, as well as the IGF binding has been shown to promote angiogenesis and positively regulate expression of other proangiogenic molecules.[61] PEDF, or Serpin, whose expression can be found in the HA functionalized hydrogels, seems to be an antiangiogenic factor, inhibiting VEGF and HGF activity. However, PEDF action is very complex, depending on the differential phosphorylation, and some forms have been reported to neutralize the antiangiogenic activity.[62] Further clarification on this topic is needed to draw more specific conclusions. Interestingly, HA molecular weight dependent differences are found on endostatin, which is a fragment of COLXVIII generated by MMP-9 cleavage, but not by MMP-2.[50] Therefore, as anticipated by zymogram analysis, endostatin was detected only for the HMW HA and GelMA samples, being absent in the LMW HA formulation. Studies have linked it to the inhibition of ECs proliferation and angiogenesis by blocking VEGF interaction with its receptor, KDR, and therefore constraining its pathways.[63] Generally speaking, the results extrapolated from the protein release profiles were consistent with the previous findings, with several of the identified proteins in the HA functionalized formulations, particularly of LMW, being linked with pro-angiogenesis mechanisms.

Overall, we were able to ascertain that LMW and HMW HA immobilization in fact influences EC behavior at different levels. LMW A-HA functionalized hydrogels were able to increase EC proliferation, metabolic activity, and migration. Moreover, LMW A-HA functionalization activates CD44/ERK1/2 signaling, MMP expression and promotes a pro-angiogenic paracrine signaling in HUVEC/hDPC cocultures. In this sense, this particular HA functionalization can be advantageous in several TE applications as a pro-angiogenesis cue, increasing the vascularization potential of other materials or systems.

5. CONCLUSIONS

The influence of HA molecular weight on the angiogenesis process has been the target of several studies with controversial results. This work reports on the successful development of a system consisting of an HA immobilization strategy onto a hydrogel substrate that showed an overall improvement of HUVEC performance, which worked as an angiogenesis inducer.

The application of LMW A-HA functionalization in other materials to stimulate angiogenic responses may contribute to improved TE and regenerative medicine strategies and assist a biocompatible solution to address the ever-present vascularization issue in engineering large functional tissue substitutes.

■ ASSOCIATED CONTENT

Supporting Information

The Supporting Information is available free of charge at https://pubs.acs.org/doi/10.1021/acsabm.1c00291.

FTIR and ^{1}H NMR spectra and chemical characterization of the modified polymers; GPC chromatograms; cell viability and proliferation assays for optimization of HA immobilization; representative micrographs of HUVECs morphology at different concentrations of A-HA solutions; total protein concentration in the condition media of HUVECs seeded on GelMA hydrogels simple and functionalized with LMW and HMW A-HA; and complete angiogenic protein profile of conditioned

https://doi.org/10.1021/acsabm.1c00291
ACS Appl. Bio Mater. 2021, 4, 6023−6035

medium obtained from hDPCs/HUVECs cocultures at day 7 (PDF)

AUTHOR INFORMATION

Corresponding Authors

Pedro S. Babo − *3B's Research Group, I3Bs − Research Institute on Biomaterials, Biodegradables and Biomimetics, University of Minho, Headquarters of the European Institute of Excellence on Tissue Engineering and Regenerative Medicine, 4805-017 Barco, Guimarães, Portugal; ICVS/3B's−PT Government Associate Laboratory, Braga/Guimarães 4710-057, Portugal;* orcid.org/0000-0003-4347-599X; Email: pedrombabo@gmail.com

Manuela E. Gomes − *3B's Research Group, I3Bs − Research Institute on Biomaterials, Biodegradables and Biomimetics, University of Minho, Headquarters of the European Institute of Excellence on Tissue Engineering and Regenerative Medicine, 4805-017 Barco, Guimarães, Portugal; ICVS/3B's−PT Government Associate Laboratory, Braga/Guimarães 4710-057, Portugal*; Email: megomes@i3bs.uminho.pt

Authors

Ana L. Silva − *3B's Research Group, I3Bs − Research Institute on Biomaterials, Biodegradables and Biomimetics, University of Minho, Headquarters of the European Institute of Excellence on Tissue Engineering and Regenerative Medicine, 4805-017 Barco, Guimarães, Portugal; ICVS/3B's−PT Government Associate Laboratory, Braga/Guimarães 4710-057, Portugal*

Márcia T. Rodrigues − *3B's Research Group, I3Bs − Research Institute on Biomaterials, Biodegradables and Biomimetics, University of Minho, Headquarters of the European Institute of Excellence on Tissue Engineering and Regenerative Medicine, 4805-017 Barco, Guimarães, Portugal; ICVS/3B's−PT Government Associate Laboratory, Braga/Guimarães 4710-057, Portugal*

Ana I. Gonçalves − *3B's Research Group, I3Bs − Research Institute on Biomaterials, Biodegradables and Biomimetics, University of Minho, Headquarters of the European Institute of Excellence on Tissue Engineering and Regenerative Medicine, 4805-017 Barco, Guimarães, Portugal; ICVS/3B's−PT Government Associate Laboratory, Braga/Guimarães 4710-057, Portugal*

Ramon Novoa-Carballal − *3B's Research Group, I3Bs − Research Institute on Biomaterials, Biodegradables and Biomimetics, University of Minho, Headquarters of the European Institute of Excellence on Tissue Engineering and Regenerative Medicine, 4805-017 Barco, Guimarães, Portugal; ICVS/3B's−PT Government Associate Laboratory, Braga/Guimarães 4710-057, Portugal;* orcid.org/0000-0003-0422-8048

Ricardo A. Pires − *3B's Research Group, I3Bs − Research Institute on Biomaterials, Biodegradables and Biomimetics, University of Minho, Headquarters of the European Institute of Excellence on Tissue Engineering and Regenerative Medicine, 4805-017 Barco, Guimarães, Portugal; ICVS/3B's−PT Government Associate Laboratory, Braga/Guimarães 4710-057, Portugal;* orcid.org/0000-0002-9197-0138

Jeroen Rouwkema − *Department of Biomechanical Engineering, Faculty of Engineering Technology, University of Twente, 7500 AE Enschede, The Netherlands;* orcid.org/0000-0001-9666-9064

Rui L. Reis − *3B's Research Group, I3Bs − Research Institute on Biomaterials, Biodegradables and Biomimetics, University of Minho, Headquarters of the European Institute of Excellence on Tissue Engineering and Regenerative Medicine, 4805-017 Barco, Guimarães, Portugal; ICVS/3B's−PT Government Associate Laboratory, Braga/Guimarães 4710-057, Portugal*

Complete contact information is available at: https://pubs.acs.org/10.1021/acsabm.1c00291

Author Contributions

A.L.S.: Investigation, formal analysis, validation, writing—original draft preparation; P.S.B.: conceptualization, methodology, investigation, formal analysis, validation, writing—review and editing; M.T.R.: investigation, writing—review and editing; AI.G.: investigation, validation, writing—review and editing; R.N.-C.: investigation, formal analysis, validation, writing—review and editing; R.A.P.: investigation, writing—review and editing; J.R.: supervision; R.L.R.: supervision; and M.E.G.: supervision, funding acquisition, writing—review and editing. All authors have approved the final version of the manuscript.

Funding

This work was supported by Norte Portugal Regional Operational Program (NORTE-01−0145-FEDER-000021) and InjecTE—Injectable biomaterials for dental tissue engineering—Project ID: 287953, financed by Norwegian Research Council (NFR) under program NANO2021.

Notes

The authors declare no competing financial interest.

ACKNOWLEDGMENTS

R.A.P. acknowledges ERA Chair Grant agreement No 668983; P.S.B. acknowledges the project FOOD4CELLS (PTDC/CTM-BIO/4706/2014-POCI-01-0145-FEDER 016716) for his postdoc grant.

ABBREVIATIONS

AFM, atomic force microscopy
A-HA, aldehyde-functionalized HA
ANOVA, analyses of variance
AREG, amphiregulin
BLAST, basic local alignment search tool
BSA, bovine serum albumin
CADH5, cadherin 5
CD31, cluster of differentiation 31
CD44, cluster of differentiation 44
cDNA, cDNA
COLXVIII, endostatin/collagen XVIII
DAPI, 4′,6-diamidino-2-phenylindole
DMEM, Dulbecco's modified Eagle's medium
ECM, extracellular matrix
ECs, endothelial cells
EDC, 1-ethyl-3-(3-(dimethylamino)propyl) carbodiimide
EDN1, endothelin-1
ENG, endoglin
ERK, extracellular regulated kinases
FBS, fetal bovine serum
GelMA, gelatin methacrylate
GPC, gel permeation chromatography
HA, hyaluronic acid
hDPCs, human dental pulp cells
HMW, high molecular weight
HUVECs, human umbilical vein endothelial cells
IBP, insulin-like growth factor-binding protein
KDR, kinase insert domain receptor

https://doi.org/10.1021/acsabm.1c00291
ACS Appl. Bio Mater. 2021, 4, 6023−6035

LMW, low molecular weight
LS, light scattering
MMP, metalloproteinase
M_w, molecular weight
NMR, nuclear magnetic resonance
PBS, phosphate buffered saline
PDI, polydispersity index
PDMS, polydimethylsiloxane
PECAM-1, platelet endothelial cell adhesion molecule
PEDF, pigment epithelium-derived factor
RHAMM, receptor for hyaluronan mediated motility
RI, refraction index
RNA, ribonucleic acid
rtPCR, real time polymerase chain reaction
SDS, sodium dodecyl sulfate
SphK, sphingosine kinase
SPR, surface plasmon resonance
TE, tissue engineering
TEMPO, (2,2,6,6-Tetramethylpiperidin-1-yl)oxyl or (2,2,6,6-tetramethylpiperidin-1-yl)oxidanyl
TGF, transforming growth factor
TIMP-1, metalloproteinase inhibitor-1
UV, ultraviolet
VEGF, vascular endothelial growth factor
VEGFR2, VEGF receptor 2

REFERENCES

(1) Rouwkema, J.; Rivron, N. C.; van Blitterswijk, C. A. Vascularization in Tissue Engineering. *Trends Biotechnol.* **2008**, *26* (8), 434−441.
(2) Jain, R. K.; Au, P.; Tam, J.; Duda, D. G.; Fukumura, D. Engineering Vascularized Tissue. *Nat. Biotechnol.* **2005**, *23* (7), 821−823.
(3) Oliveira, S. M.; Pirraco, R. P.; Marques, A. P.; Santo, V. E.; Gomes, M. E.; Reis, R. L.; Mano, J. F. Platelet Lysate-Based pro-Angiogenic Nanocoatings. *Acta Biomater.* **2016**, *32*, 129−137.
(4) Lovett, M.; Lee, K.; Edwards, A.; Kaplan, D. L. Vascularization Strategies for Tissue Engineering. *Tissue Eng., Part B* **2009**, *15* (3), 353−370.
(5) Novosel, E. C.; Kleinhans, C.; Kluger, P. J. Vascularization Is the Key Challenge in Tissue Engineering. *Adv. Drug Delivery Rev.* **2011**, *63* (4−5), 300−311.
(6) Mongiat, M.; Andreuzzi, E.; Tarticchio, G.; Paulitti, A. Extracellular Matrix, a Hard Player in Angiogenesis. *Int. J. Mol. Sci.* **2016**, *17* (11), 1822.
(7) Toole, B. P.; Yu, Q.; Underhill, C. B. Hyaluronan and Hyaluronan-Binding Proteins: Probes for Specific Detection. In *Proteoglycan Protocols*; Humana Press: Totowa, NJ, pp 479−485 DOI: 10.1385/1-59259-209-0:479.
(8) Wang, Y. Z.; Cao, M. L.; Liu, Y. W.; He, Y. Q.; Yang, C. X.; Gao, F. CD44 Mediates Oligosaccharides of Hyaluronan-Induced Proliferation, Tube Formation and Signal Transduction in Endothelial Cells. *Exp. Biol. Med.* **2011**, *236* (1), 84−90.
(9) Slevin, M.; Krupinski, J.; Gaffney, J.; Matou, S.; West, D.; Delisser, H.; Savani, R. C.; Kumar, S. Hyaluronan-Mediated Angiogenesis in Vascular Disease: Uncovering RHAMM and CD44 Receptor Signaling Pathways. *Matrix Biol.* **2007**, *26* (1), 58−68.
(10) Ibrahim, S.; Ramamurthi, A. Hyaluronic Acid Cues for Functional Endothelialization of Vascular Constructs. *J. Tissue Eng. Regener. Med.* **2008**, *2* (1), 22−32.
(11) Cui, X.; Xu, H.; Zhou, S.; Zhao, T.; Liu, A.; Guo, X.; Tang, W.; Wang, F. Evaluation of Angiogenic Activities of Hyaluronan Oligosaccharides of Defined Minimum Size. *Life Sci.* **2009**, *85* (15−16), 573−577.
(12) Sapudom, J.; Ullm, F.; Martin, S.; Kalbitzer, L.; Naab, J.; Möller, S.; Schnabelrauch, M.; Anderegg, U.; Schmidt, S.; Pompe, T. Molecular Weight Specific Impact of Soluble and Immobilized Hyaluronan on CD44 Expressing Melanoma Cells in 3D Collagen Matrices. *Acta Biomater.* **2017**, *50*, 259−270.
(13) Loessner, D.; Meinert, C.; Kaemmerer, E.; Martine, L. C.; Yue, K.; Levett, P. A.; Klein, T. J.; Melchels, F. P. W.; Khademhosseini, A.; Hutmacher, D. W. Functionalization, Preparation and Use of Cell-Laden Gelatin Methacryloyl−Based Hydrogels as Modular Tissue Culture Platforms. *Nat. Protoc.* **2016**, *11* (4), 727−746.
(14) Yue, K.; Trujillo-de Santiago, G.; Alvarez, M. M.; Tamayol, A.; Annabi, N.; Khademhosseini, A. Synthesis, Properties, and Biomedical Applications of Gelatin Methacryloyl (GelMA) Hydrogels. *Biomaterials* **2015**, *73*, 254−271.
(15) Deng, Y.; Ren, J.; Chen, G.; Li, G.; Wu, X.; Wang, G.; Gu, G.; Li, J. Injectable in Situ Cross-Linking Chitosan-Hyaluronic Acid Based Hydrogels for Abdominal Tissue Regeneration. *Sci. Rep.* **2017**, *7* (1), 2699.
(16) Šedová, P.; Buffa, R.; Kettou, S.; Huerta-Angeles, G.; Hermannová, M.; Leierová, V.; Šmejkalová, D.; Moravcová, M.; Velebný, V. Preparation of Hyaluronan Polyaldehyde—a Precursor of Biopolymer Conjugates. *Carbohydr. Res.* **2013**, *371*, 8−15.
(17) Mero, A.; Pasqualin, M.; Campisi, M.; Renier, D.; Pasut, G. Conjugation of Hyaluronan to Proteins. *Carbohydr. Polym.* **2013**, *92* (2), 2163−2170.
(18) Han, L.; Xu, J.; Lu, X.; Gan, D.; Wang, Z.; Wang, K.; Zhang, H.; Yuan, H.; Weng, J. Biohybrid Methacrylated Gelatin/Polyacrylamide Hydrogels for Cartilage Repair. *J. Mater. Chem. B* **2017**, *5* (4), 731−741.
(19) Almeida, L. D. F.; Babo, P. S.; Silva, C. R.; Rodrigues, M. T.; Hebling, J.; Reis, R. L.; Gomes, M. E. Hyaluronic Acid Hydrogels Incorporating Platelet Lysate Enhance Human Pulp Cell Proliferation and Differentiation. *J. Mater. Sci.: Mater. Med.* **2018**, *29* (6) DOI: 10.1007/s10856-018-6088-7.
(20) Ren, Z.; Chen, J.; Khalil, R. A. *Methods Mol. Biol.* **2017**, *1626*, 79−102.
(21) Rouwkema, J.; Khademhosseini, A. Vascularization and Angiogenesis in Tissue Engineering: Beyond Creating Static Networks. *Trends Biotechnol.* **2016**, *34* (9), 733−745.
(22) Cheresh, D. A.; Stupack, D. G. Regulation of Angiogenesis: Apoptotic Cues from the ECM. *Oncogene* **2008**, *27* (48), 6285−6298.
(23) Yang, C.; Cao, M.; Liu, H.; He, Y.; Xu, J.; Du, Y.; Liu, Y.; Wang, W.; Cui, L.; Hu, J.; Gao, F. The High and Low Molecular Weight Forms of Hyaluronan Have Distinct Effects on CD44 Clustering. *J. Biol. Chem.* **2012**, *287* (51), 43094−43107.
(24) Kouvidi, K.; Berdiaki, A.; Nikitovic, D.; Katonis, P.; Afratis, N.; Hascall, V. C.; Karamanos, N. K.; Tzanakakis, G. N. Role of Receptor for Hyaluronic Acid-Mediated Motility (RHAMM) in Low Molecular Weight Hyaluronan (LMWHA)-Mediated Fibrosarcoma Cell Adhesion. *J. Biol. Chem.* **2011**, *286* (44), 38509−38520.
(25) Pardue, E. L.; Ibrahim, S.; Ramamurthi, A. Role of Hyaluronan in Angiogenesis and Its Utility to Angiogenic Tissue Engineering. *Organogenesis* **2008**, *4* (4), 203−214.
(26) Cyphert, J. M.; Trempus, C. S.; Garantziotis, S. Size Matters: Molecular Weight Specificity of Hyaluronan Effects in Cell Biology. *Int. J. Cell Biol.* **2015**, *2015*, 1−8.
(27) Banerji, S.; Wright, A. J.; Noble, M.; Mahoney, D. J.; Campbell, I. D.; Day, A. J.; Jackson, D. G. Structures of the Cd44−Hyaluronan Complex Provide Insight into a Fundamental Carbohydrate-Protein Interaction. *Nat. Struct. Mol. Biol.* **2007**, *14* (3), 234−239.
(28) Kessler, L.; Gehrke, S.; Winnefeld, M.; Huber, B.; Hoch, E.; Walter, T.; Wyrwa, R.; Schnabelrauch, M.; Schmidt, M.; Kückelhaus, M.; Lehnhardt, M.; Hirsch, T.; Jacobsen, F. Methacrylated Gelatin/Hyaluronan-Based Hydrogels for Soft Tissue Engineering. *J. Tissue Eng.* **2017**, *8*, 204173141774415.
(29) Camci-Unal, G.; Cuttica, D.; Annabi, N.; Demarchi, D.; Khademhosseini, A. Synthesis and Characterization of Hybrid Hyaluronic Acid-Gelatin Hydrogels. *Biomacromolecules* **2013**, *14* (4), 1085−1092.
(30) Klotz, B. J.; Gawlitta, D.; Rosenberg, A. J. W. P.; Malda, J.; Melchels, F. P. W. Gelatin-Methacryloyl Hydrogels: Towards Biofabrication-Based Tissue Repair. *Trends Biotechnol.* **2016**, *34* (5), 394−407.

https://doi.org/10.1021/acsabm.1c00291
ACS Appl. Bio Mater. 2021, 4, 6023−6035

(31) Domingues, R. M. A.; Silva, M.; Gershovich, P.; Betta, S.; Babo, P.; Caridade, S. G.; Mano, J. F.; Motta, A.; Reis, R. L.; Gomes, M. E. Development of Injectable Hyaluronic Acid/Cellulose Nanocrystals Bionanocomposite Hydrogels for Tissue Engineering Applications. *Bioconjugate Chem.* **2015**, *26* (8), 1571−1581.
(32) Tsanaktsidou, E.; Kammona, O.; Kiparissides, C. On the Synthesis and Characterization of Biofunctional Hyaluronic Acid Based Injectable Hydrogels for the Repair of Cartilage Lesions. *Eur. Polym. J.* **2019**, *114*, 47−56.
(33) Eastoe, J. E. The Amino Acid Composition of Mammalian Collagen and Gelatin. *Biochem. J.* **1955**, *61* (4), 589−600.
(34) Kirsch, M.; Birnstein, L.; Pepelanova, I.; Handke, W.; Rach, J.; Seltsam, A.; Scheper, T.; Lavrentieva, A. Gelatin-Methacryloyl (GelMA) Formulated with Human Platelet Lysate Supports Mesenchymal Stem Cell Proliferation and Differentiation and Enhances the Hydrogel's Mechanical Properties. *Bioengineering* **2019**, *6* (3), 76.
(35) Nichol, J. W.; Koshy, S. T.; Bae, H.; Hwang, C. M.; Yamanlar, S.; Khademhosseini, A. Cell-Laden Microengineered Gelatin Methacrylate Hydrogels. *Biomaterials* **2010**, *31* (21), 5536−5544.
(36) Kujawa, P.; Moraille, P.; Sanchez, J.; Badia, A.; Winnik, F. M. Effect of Molecular Weight on the Exponential Growth and Morphology of Hyaluronan/Chitosan Multilayers: A Surface Plasmon Resonance Spectroscopy and Atomic Force Microscopy Investigation. *J. Am. Chem. Soc.* **2005**, *127* (25), 9224−9234.
(37) Amorim, S.; Pashkuleva, I.; Reis, C. A.; Reis, R. L.; Pires, R. A. Tunable Layer-by-Layer Films Containing Hyaluronic Acid and Their Interactions with CD44. *J. Mater. Chem. B* **2020**, *8*, 3880.
(38) Chen, Y.-C.; Lin, R.-Z.; Qi, H.; Yang, Y.; Bae, H.; Melero-Martin, J. M.; Khademhosseini, A. Functional Human Vascular Network Generated in Photocrosslinkable Gelatin Methacrylate Hydrogels. *Adv. Funct. Mater.* **2012**, *22* (10), 2027−2039.
(39) Amorim, S.; da Costa, D. S.; Freitas, D.; Reis, C. A.; Reis, R. L.; Pashkuleva, I.; Pires, R. A. Molecular Weight of Surface Immobilized Hyaluronic Acid Influences CD44-Mediated Binding of Gastric Cancer Cells. *Sci. Rep.* **2018**, *8* (1), 16058.
(40) Vanderhooft, J. L.; Alcoutlabi, M.; Magda, J. J.; Prestwich, G. D. Rheological Properties of Cross-Linked Hyaluronan-Gelatin Hydrogels for Tissue Engineering. *Macromol. Biosci.* **2009**, *9* (1), 20−28.
(41) Tanimura, S.; Takeda, K. ERK Signalling as a Regulator of Cell Motility. *J. Biochem.* **2017**, *162* (3), 145−154.
(42) Fincham, V. J. Active ERK/MAP Kinase Is Targeted to Newly Forming Cell-Matrix Adhesions by Integrin Engagement and v-Src. *EMBO J.* **2000**, *19* (12), 2911−2923.
(43) Shabafrooz, V.; Mozafari, M.; Köhler, G. A.; Assefa, S.; Vashaee, D.; Tayebi, L. The Effect of Hyaluronic Acid on Biofunctionality of Gelatin-Collagen Intestine Tissue Engineering Scaffolds. *J. Biomed. Mater. Res., Part A* **2014**, *102* (9), 3130−3139.
(44) Abhinand, C. S.; Raju, R.; Soumya, S. J.; Arya, P. S.; Sudhakaran, P. R. VEGF-A/VEGFR2 Signaling Network in Endothelial Cells Relevant to Angiogenesis. *J. Cell Commun. Signal.* **2016**, *10* (4), 347−354.
(45) Yu, Q.; Stamenkovic, I. Cell Surface-Localized Matrix Metalloproteinase-9 Proteolytically Activates TGF-Beta and Promotes Tumor Invasion and Angiogenesis. *Genes Dev.* **2000**, *14* (2), 163−176.
(46) Belotti, D.; Paganoni, P.; Manenti, L.; Garofalo, A.; Marchini, S.; Taraboletti, G.; Giavazzi, R. Matrix Metalloproteinases (MMP9 and MMP2) Induce the Release of Vascular Endothelial Growth Factor (VEGF) by Ovarian Carcinoma Cells. *Cancer Res.* **2003**, *63* (17), 5224−5229.
(47) Lee, S.; Jilani, S. M.; Nikolova, G. V.; Carpizo, D.; Iruela-Arispe, M. L. Processing of VEGF-A by Matrix Metalloproteinases Regulates Bioavailability and Vascular Patterning in Tumors. *J. Cell Biol.* **2005**, *169* (4), 681−691.
(48) KVANTA, A.; SARMAN, S.; FAGERHOLM, P.; SEREGARD, S.; STEEN, B. Expression of Matrix Metalloproteinase-2 (MMP-2) and Vascular Endothelial Growth Factor (VEGF) in Inflammation-Associated Corneal Neovascularization. *Exp. Eye Res.* **2000**, *70* (4), 419−428.
(49) Mauceri, H. J.; Seetharam, S.; Beckett, M. A.; Lee, J. Y.; Gupta, V. K.; Gately, S.; Stack, M. S.; Brown, C. K.; Swedberg, K.; Kufe, D. W.; Weichselbaum, R. R. Tumor Production of Angiostatin Is Enhanced after Exposure to TNF-? *Int. J. Cancer* **2002**, *97* (4), 410−415.
(50) Ferreras, M.; Felbor, U.; Lenhard, T.; Olsen, B. R.; Delaissé, J.-M. Generation and Degradation of Human Endostatin Proteins by Various Proteinases. *FEBS Lett.* **2000**, *486* (3), 247−251.
(51) Tao, H.; Han, Z.; Han, Z. C.; Li, Z. Proangiogenic Features of Mesenchymal Stem Cells and Their Therapeutic Applications. *Stem Cells Int.* **2016**, *2016*, 1−11.
(52) Kehl, D.; Generali, M.; Mallone, A.; Heller, M.; Uldry, A.-C.; Cheng, P.; Gantenbein, B.; Hoerstrup, S. P.; Weber, B. Proteomic Analysis of Human Mesenchymal Stromal Cell Secretomes: A Systematic Comparison of the Angiogenic Potential. *npj Regen. Med.* **2019**, *4* (1), 8.
(53) Gharaei, M. A.; Xue, Y.; Mustafa, K.; Lie, S. A.; Fristad, I. Human Dental Pulp Stromal Cell Conditioned Medium Alters Endothelial Cell Behavior. *Stem Cell Res. Ther.* **2018**, *9* (1), 69.
(54) Silva, C. R.; Babo, P. S.; Gulino, M.; Costa, L.; Oliveira, J. M.; Silva-Correia, J.; Domingues, R. M. A.; Reis, R. L.; Gomes, M. E. Injectable and Tunable Hyaluronic Acid Hydrogels Releasing Chemotactic and Angiogenic Growth Factors for Endodontic Regeneration. *Acta Biomater.* **2018**, *77*, 155−171.
(55) Dissanayaka, W. L.; Zhan, X.; Zhang, C.; Hargreaves, K. M.; Jin, L.; Tong, E. H. Y. Coculture of Dental Pulp Stem Cells with Endothelial Cells Enhances Osteo-/Odontogenic and Angiogenic Potential In Vitro. *J. Endod.* **2012**, *38* (4), 454−463.
(56) Heloterä, H.; Alitalo, K. The VEGF Family, the Inside Story. *Cell* **2007**, *130* (4), 591−592.
(57) Thurston, G. Complementary Actions of VEGF and Angiopoietin-1 on Blood Vessel Growth and Leakage*. *J. Anat.* **2002**, *200* (6), 575−580.
(58) Rescan, C.; Coutant, A.; Talarmin, H.; Theret, N.; Glaise, D.; Guguen-Guillouzo, C.; Baffet, G. Mechanism in the Sequential Control of Cell Morphology and S Phase Entry by Epidermal Growth Factor Involves Distinct MEK/ERK Activations. *Mol. Biol. Cell* **2001**, *12* (3), 725−738.
(59) Zlot, C.; Ingle, G.; Hongo, J.; Yang, S.; Sheng, Z.; Schwall, R.; Paoni, N.; Wang, F.; Peale, F. V.; Gerritsen, M. E. Stanniocalcin 1 Is an Autocrine Modulator of Endothelial Angiogenic Responses to Hepatocyte Growth Factor. *J. Biol. Chem.* **2003**, *278* (48), 47654−47659.
(60) Granata, R.; Trovato, L.; Garbarino, G.; Taliano, M.; Ponti, R.; Sala, G.; Ghidoni, R.; Ghigo, E. Dual Effects of IGFBP-3 on Endothelial Cell Apoptosis and Survival: Involvement of the Sphingolipid Signaling Pathways. *FASEB J.* **2004**, *18* (12), 1456−1458.
(61) GRANATA, R.; TROVATO, L.; LUPIA, E.; SALA, G.; SETTANNI, F.; CAMUSSI, G.; GHIDONI, R.; GHIGO, E. Insulin-like Growth Factor Binding Protein-3 Induces Angiogenesis through IGF-I- and SphK1-Dependent Mechanisms. *J. Thromb. Haemostasis* **2007**, *5* (4), 835−845.
(62) Maik-Rachline, G.; Seger, R. Variable Phosphorylation States of Pigment-Epithelium−Derived Factor Differentially Regulate Its Function. *Blood* **2006**, *107* (7), 2745−2752.
(63) Kim, Y.-M.; Hwang, S.; Kim, Y.-M.; Pyun, B.-J.; Kim, T.-Y.; Lee, S.-T.; Gho, Y. S.; Kwon, Y.-G. Endostatin Blocks Vascular Endothelial Growth Factor-Mediated Signaling via Direct Interaction with KDR/Flk-1. *J. Biol. Chem.* **2002**, *277* (31), 27872−27879.

https://doi.org/10.1021/acsabm.1c00291
ACS Appl. Bio Mater. 2021, 4, 6023−6035